IN-SILICO STUDY OF ADMET PROPERTIES, MOLECULAR DOCKING AND MOLECULAR DYNAMICS OF POTENTIAL INHIBITORS OF New Delhi metallo-β-lactamase (NDM-1)

Eduvan Valencia[1*], Wilson Olarte[2]

Received for review M-D-A, accepted M-D-A, final version M-D-A

Abstract: The metalloenzyme New Delhi Metallo-β-lactamase-1 (NDM-1), as well as its reported variants, present multidrug resistance to different antibiotics for the treatment of infectious diseases, due to its ability to hydrolyze a large number of β-lactam compounds such as carbapenems, a factor that has an impact on microbial resistance, which is a worldwide concern. The present work is based on a previous study of the ADMET properties of 56 potential inhibitors of the NDM-1 enzyme, of which 22 compounds showed promising oral bioavailability and toxicity values; These compounds present in their structure ethylenediamine derivatives, N,N',N''-triacetate-1,4,7-triazacyclonane, phosphonic acid mercapto esters, sulfur-containing carboxylic acids, dipicolinic acid, cyclic borate, chromones, natural compounds and their thioamide derivatives. For this group of selected molecules, molecular docking was performed with AutoDock4 and AutoDock4Zn, finding small differences between the force fields applied by each program whose docking energy results were (kcal/mol): AutoDock4 of -12.88 for M26 and -10.6 for M25, as well as -12.84 for M26 and -11.21 for M25 with AutoDock4Zn. Finally, 10ns molecular dynamics was performed for the best docking found (M26), with GROMACS software, obtaining acceptable ranges of RMSD and RMSF determining the best approximation to the possible real behavior of the molecular complex analyzed.

Keywords: NDM-1; ADMET Properties; Molecular Coupling; Molecular Dynamics.

1. INTRODUCTION

In recent years, there has been growing concern in the world in the different public and global health systems for the treatment of some infectious diseases, mainly caused by bacteria multiresistant to antibiotics for general use, such as β-lactams, which have been widely used for decades due to their high efficacy, affordability and low toxicity (Rehman, M. et al., 2019). The aforementioned poses a latent risk of a worldwide pandemic, which would put the health systems of the various countries in crisis (Haque, et al., 2022). This may be due, to a large extent, to the indiscriminate use of antibiotics (in some countries), by self-prescription in humans and animals, which has caused microorganisms in their processes of mutation and therefore evolution, to create resistance mechanisms, among which is most frequently the

1 Secretaría de Educación Distrital de Bogotá..

2 Secretaría de Educación y Cultura de Cundinamarca.

* *Autor correspondencia: edvalenciac@unal.edu.co*

production of ß-lactamase enzymes that hydrolyze the nucleus of the ß-lactam ring of conventionally used antibiotics, inhibiting their bactericidal or bacteriostatic action (Suarez et al., 2009; Yacoby et al., 2007; Cruz et al., 2010; Yang et al., 2015; Liu et al., 2015). Some of the bacteria that have shown resistance to most antibiotics by the production of acquired carbapenemases are of the non-fermentative Gram-negative type, such as those published by WHO in February 2017 as pathogens to be prioritized and for which new antibiotics are urgently needed. Among bacteria include the following: Acinetobacter, Pseudomonas and members of the Enterobacteriaceae family such as Klebsiella spp, Serratia, Proteus, E. coli and Enterobacter spp (Kar, B. et al., 2023), which undoubtedly and as mentioned in previous lines, pose a worrying public health problem globally due to their rapid dissemination and high resistance in the hospital environment (Queenan et al., 2007; Papp et al., 2011; Gonzalez et al., 2015), being the cause of approximately 1.27 million deaths in 2019 associated with multidrug resistance to various antimicrobials (Murray et al., 2022). When patients present infections by resistant bacteria, broad-spectrum antibiotics such as carbapenemics are used, which are used as the last line of defense (Ariza et al., 2013; Deshpande et al., 2010), since they are more stable against β-lactamase enzymes and have a broader spectrum than other β-lactam antibiotics, (Salih, T., & Ali, P. G., 2023); the drawback is that such drugs are not able to exert their therapeutic action, due to the appearance of carbapenemase type enzymes such as NDM (New Delhi Metalobetalactamase) in microorganisms that specialize in the inactivation of drugs, causing the blockage of their pharmacological function (Morales et al., 2014). For this reason, research groups in microbiology and medicinal chemistry, among others, have focused their efforts on searching for, creating or identifying new inhibitors that lack the β-lactam ring and that better circumvent these defense mechanisms and show a good oral bioavailability and toxicity profile (Alcaide et al., 2004; Haque, et al., 2023).

As for the structure of the NDM-1 enzyme, it consists of a single chain of 270 residues, with a signal peptide of 28 amino acids at the N-terminal end. The protein can move into the periplasmic space and even into the outer membrane of Gram-negative bacteria to hydrolyze β-lactam antibiotics (Salih, T., & Ali, P. G., 2023). The active site of the metalloprotein, is located around two Zn2+ ions which is surrounded by the amino acids His-120, His-122, Asp-124, His-189, Cys-208 and His-250. One of the zinc ions (Zn2+) shows tetrahedral coordination formed by binding to the amino acids His-120, His-122, His-189 and one those of the hydroxyl groups of the amino acid Asp-124 (Bebrone., 2007; Guo et al., 2011).

As for the second Zn2+ cation, it has been found to form a trigonal pyramidal coordination involving one of the hydroxyl groups of Asp-124 and the amino acids Cys-208 and His-250. Figure 1 shows a representation of the active site of NDM-1, highlighting the binding of the two catalytic zinc ions, their geometries and the

respective binding distances between them, the solvent and the amino acids with which they coordinate.

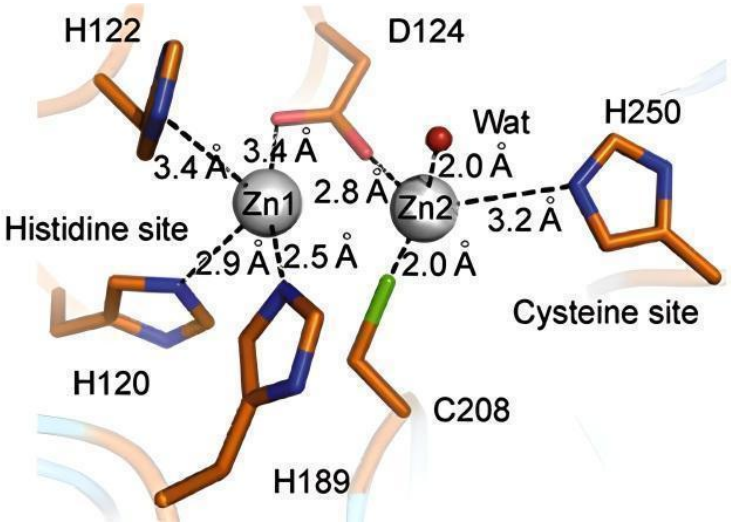

Figure 1. View of the active site of the MBL NDM-1 enzyme. Source: Guo et al., 2011.

The two zinc ions interact with each other at a distance of 3.2Å and are bridged in turn by the amino acid Asp-124. A Zn2+, in the vicinity of the so-called "cysteine site", and as can be seen in Figure 1, a distance of 2Å between the oxygen of the solvent molecule and the Zn2+ ion, indicating a hydroxide bond which could serve as an attacking nucleophile on the carbonyl carbon of the ß-lactam ring (Guo et al., 2011). However, elucidation of the precise mechanism of action of NDM-1 still requires further investigation (Salih, T., & Ali, P. G., 2023).

Computer-aided drug design continues to be one of the forms of analysis commonly performed in drug discovery and development, in order to reduce costs and obtain results in less time (Etruri et al., 2021). Through in-silico assays, it is possible to predict values or estimates of descriptors or properties of interest, through approximations and probabilities, by modeling with values already published in the literature, and by analyzing the structure of the molecule (Etruri, et al., 2021). Such data give us insight into the bioavailability and biosafety profile in a rational way, and discarding those compounds that may show undesirable values, although one must be very intuitive in filtering such compounds as many molecules may have values within the optimal ranges and yet are orally inactive, while others are active despite deviating in some of these physicochemical parameters (Xiong, et al., 2021). The computational approaches needed to design potential inhibitors of metallo β-lacatamases against NDM-1 protein may improve the success of the project and reduce the cost of developing new lead molecules, as mentioned above (Salih, T., & Ali, P. G., 2023).

The present investigation was based on the evaluation, by means of in silico assays, of a group of molecules selected in a previous study, from which 22 compounds with the best oral bioavailability values and low toxicity were obtained, among which are ethylenediamine derivatives, N,N',N''-triacetate-1,4,7-triazacyclonane, mercapto esters of phosphonic acid, sulfur-containing carboxylic acids, dipicolinic acid, cyclic borate, chromones, natural compounds and their thioamide derivatives. The selected potential inhibitors were subjected to molecular docking calculations against the NDM-1 enzyme encoded in PDB 5ZGZ, using the AutoDock4 and AutoDock4$_{Zn}$ programs available in AutoDock. The compound that showed the best binding energy affinity was selected to perform a molecular dynamics (MD) simulation for 10ns, in order to establish the stability of the identified molecule and the NDM-1 complex, establishing compound M26 as a potential inhibitor of the drug target under study.

2. MATERIALS AND METHODS

Initially, the structure of the metalloenzyme NDM-1, with code 5ZGZ, was downloaded from the Protein Bank (PDB) of the RCSC, taking into account some parameters such as resolution, free R value, among others, for its selection. The ligands were taken from a previous research carried out by the authors, from which 22 possible inhibitors were chosen to be analyzed, which yielded the best values of absorption, distribution, metabolism, excretion and toxicity.

2.1. PROTEIN PREPARATION

The structure of the NDM-1 enzyme was selected from the RCSB PDB among more than 40 possible proteins, where priority was given to the lowest resolution values (5ZGZ=0.95 Å), minimum free R value (5ZGZ=0.135), number of chains (only chain A) since its action is as a monomer, percentile ranges, chain length (242 amino acids), and no mutations (Bernstein et al., 1978). The metalloenzyme was refined using the UCSF Chimera 1.17.3 software, where the water molecules and the EDO ligand (1,2-ethanediol) were eliminated; the missing residues in the crystal structure (28 amino acids) were not included for the present study. Subsequently, AutoDockTools 1.5.6 software was used, where polar hydrogens, Kollman charges (specific for amino acids) were added. The protein was saved in PDBQT format for subsequent molecular docking.

2.2. LIGAND PREPARATION

The 2D structures of the potential NDM-1 inhibitors (Fig. 2), were drawn with the MarvinSketch 23.12 program, the protonation states were calculated at pH=7.5 and saved in mol2 format with the same software. The 3D structures and their subsequent optimization were carried out with the Avogadro 1.2.0 software, where the hydrogens were added at pH=7.5 and then an energy minimization was performed using the UFF force fields for the molecules with Boron and Potassium and MMFF94 (Salih, T., & Ali, P., 2023) for the other compounds, including the reference antibiotics and saved in mol2 and PDB format. The next step was to process the ligands with AutoDockTools 1.5.6, where all the hydrogens were added, the Gasteiger charges were computed and the non-polar hydrogens were applied, the molecules were saved in PDBQT format to be used for molecular docking (Kar, B. et al., 2023).

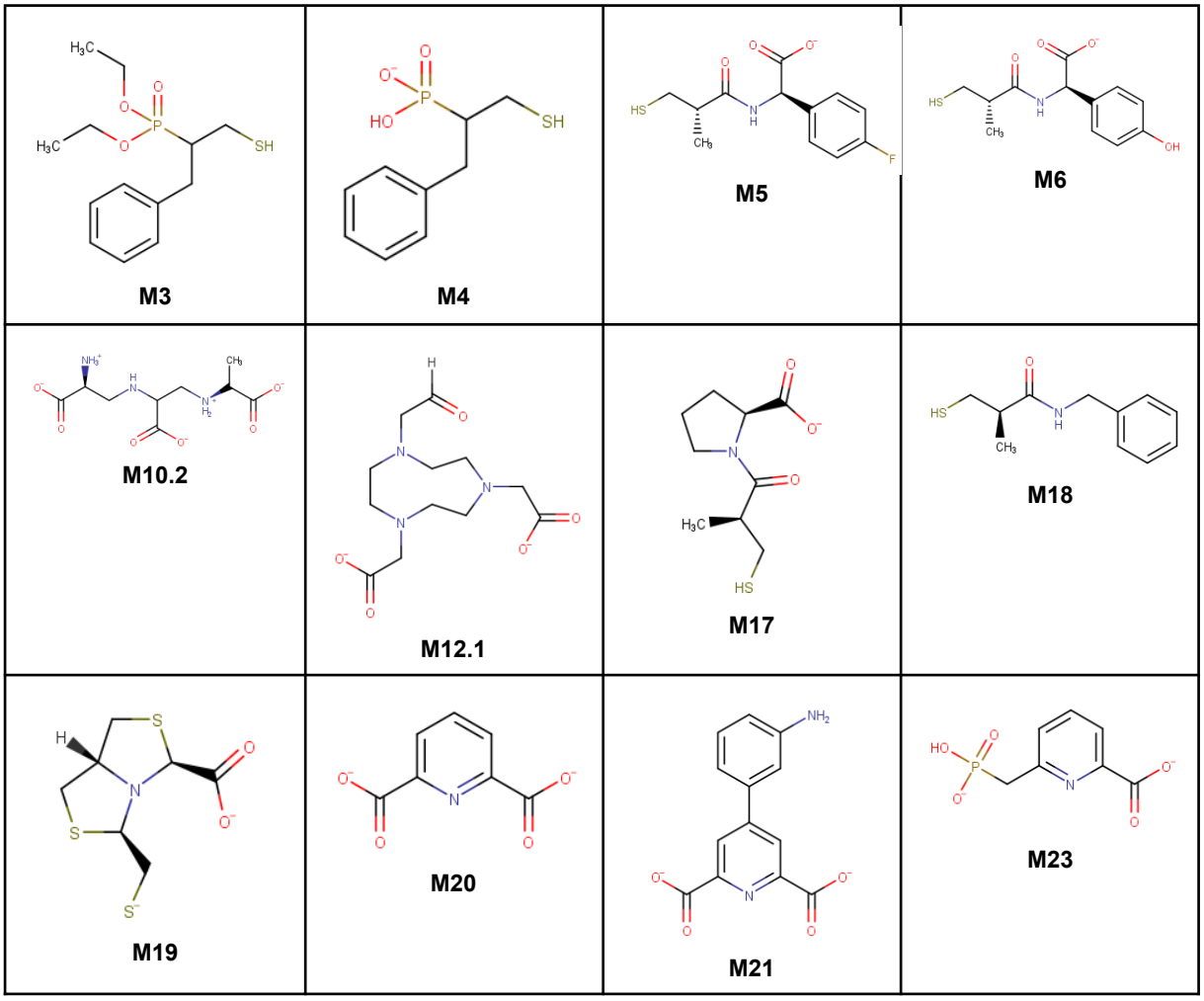

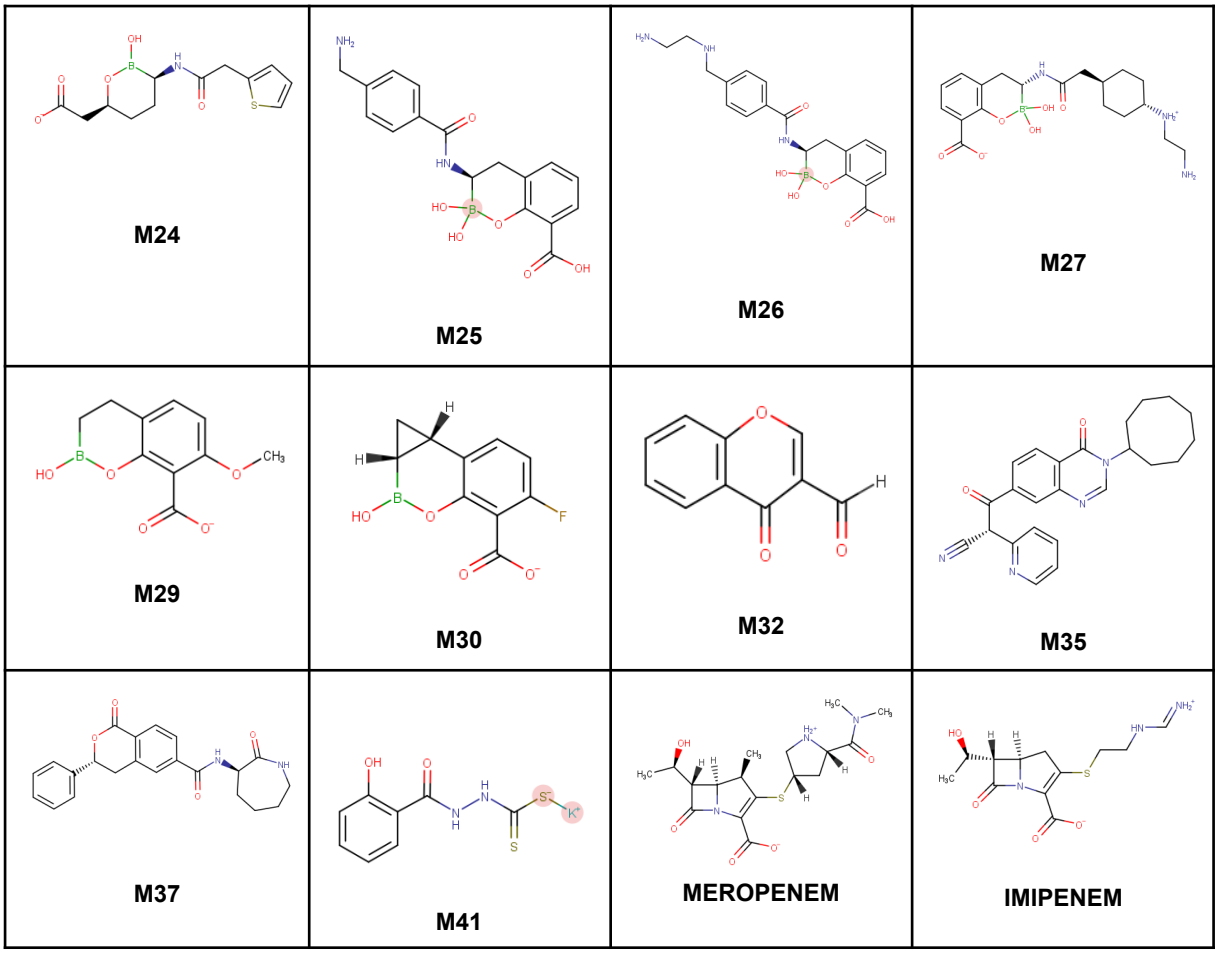

Figure 2. Structures at pH=7.5 of the 22 compounds and the 2 reference drugs.

2.3. MOLECULAR DOCKING

Molecular docking of the compounds tested, to determine the binding energy (ΔG) with the drug target, was carried out with AutoDock software, which provides a set of tools to predict how small molecules, such as substrates or drug candidates, bind to a receptor of known 3D structure (Goodsell, D. et al., 1996). From AutoDock, AutoDock4 (AutoDockTools 1.5.7) and AutoDock4Zn (AMDock 1.5.2), were used to perform the docking calculations in order to compare the values obtained between the two programs, since, AutoDock4Zn adds a specific force field for metalloproteins containing Zn atoms in their structure (Santos-Martins, D. et al., 2014). Starting from the preparation of the enzyme and ligands, the size of the GRID BOX was established, taking as reference the amino acids of the active site of the protein (Bebrone, 2007; Guo et al., 2011) and the size of the drugs and potential inhibitors, the values were: for the center, X= -4.2, Y= -5.4, Z= -16.2, for the size, X= 40, Y= 38, Z=44 Å3. Subsequently, the genetic algorithm was used with the maximum possible number of evaluations for each program (AutoDockTools= 25000000 , AMDock= 10000000), for the output file, the Lamarckian genetic algorithm was used and

Dockings were run. The conformations generated by the compounds and antibiotics were evaluated based on the binding free energy values, selecting the best value for molecular dynamics calculations.

2.4. MOLECULAR INTERACTIONS

The 3D visualization of possible hydrophobic interactions, hydrogen bonds, between the ligands and the NDM-1 enzyme was initially carried out with the AutoDockTools and PyMOL programs. For the generation of 2D docking images, LigPlot v.2.2 software was used. The above described allows us to have a detailed approximation of the possible inhibition mechanisms that the molecules under study may have against the selected pharmacological target (Kar, B. et al., 2023).

2.5. MOLECULAR DYNAMICS

Taking into account the binding free energy values for the molecular couplings of the compounds analyzed, the best confomer was selected in order to perform the molecular dynamics simulations and thus verify the stability and flexibility of the complex throughout the run. To achieve the above, the program GROMACS 2023.2 (Van Der Spoel, D. et al., 2005) was used, the simulation time was 10ns in water, using the CHARMM36-Jul 2022.ff force field. The solvation box for the protein-ligand complex was of dodecahedral structure, which contained water according to the SPC model and sodium/chloride ions were added in order to equilibrate the system.

2.6. MOLECULAR DYNAMICS TRAJECTORY

Once the MD calculations were completed, periodic boundary correction (PBC) was performed. For verification of structural stability and flexibility, root mean square deviation (RMSD) and root mean square fluctuation (RMSF) were determined, respectively, using Gromacs scripts. XmGrace (Kar, B. et al., 2023) was used for graph visualization.

3. RESULTS AND DISCUSSION

3.1. MOLECULAR DOCKING

Twenty-two compounds reported in the literature and two reference antibiotics (Meropenem and Imipenem) were docked with the NDM-1 (PDB:5ZGZ) structure, of which four (4) compounds presented the best affinity results in both Autodock4 and Autodock$_{Zn}$ docking. The binding energies of the four selected compounds, as well as their main molecular interactions, bond nature and distances, are presented in Table 1 (AutoDock4) and Table 2 (AutoDook$_{Zn}$).

Table 1. Best in-silico values of molecular docking between NDM-1 and the molecules under study, employing AutoDock4 (AutoDockTools 1.5.7).

Molecule	Molecular Interaction	Nature of the interaction	Distance (A°)	Docking binding energy (∆G) Kcal/mol
M25	M25: H-OH 303: O M25: H-OH 303: O Lys 211:HZ2-M25: O Asn 220: HD22-M25:O,O	Hydrogen bond Hydrogen bond Hydrogen bond Hydrogen bond	1.91 2.02 2.10 2.18	-10.6
M26	M26: H-OH 303: O M26: H-Glu 152: OE1 M26: H-Asp124: OD1; H-OH 303: O Asn 220: HN-M26:O Asn 220: HD22-M26:O	Hydrogen bond Hydrogen bond Hydrogen bond Hydrogen bond Hydrogen bond	2.07 1.72 2.11 1.86 1.89	-12.88
M35	Gln 123: HN-M35: N Asn 124: HN-M35: O Asn 220: HN-M35: O	Hydrogen bond Hydrogen bond Hydrogen bond	2.18 2.18 2.23	-9.02
M37	Lys 211:HZ2-M37: O Lys 211:HZ3-M37: O Asn 220: HD22-M37: O	Hydrogen bond Hydrogen bond Hydrogen bond	2.02 1.89 1.65	-9.2
MEROPENEM	Lys 211:HZ2-MEROPENEM: O Lys 211:HZ1-MEROPENEM: O Lys 211:HZ3-MEROPENEM: O Asn 220:HN-MEROPENEM: O Asn 220:HD22-MEROPENEM: O	Hydrogen bond Hydrogen bond Hydrogen bond Hydrogen bond Hydrogen bond	1.91 1.77 2.04 2.02 1.97	-9.15

Source: Self elaboration.

Table 2. Best in-silico values of molecular docking between NDM-1 and the molecules under study, using AutoDock4$_{Zn}$ (AMDock 1.5.2).

Molecule	Molecular Interaction	Nature of the interaction	Distance (A°)	Docking binding energy (∆G) Kcal/mol
M25	M25: H-OH 303: O M25: H-OH 303: O Lys 211:HZ3-M25: O Asn 220: HN-M25:O Asn 220: HD22-M25:O,O	Hydrogen bond Hydrogen bond Hydrogen bond Hydrogen bond Hydrogen bond	1.94 2.06 2.23 2.02 2.04	-11.21
M26	M26: H-OH 303: O M26: H-Glu 152: OE1 M26: H-Asp124: OD1; H-OH 303: O Asn 220: HD22-M26:O Asn 220: HN-M26:O Lys 211:HZ1-M26: O	Hydrogen bond Hydrogen bond Hydrogen bond Hydrogen bond Hydrogen bond Hydrogen bond	2.02 1.69 2.18 2.01 1.88 1.95	-12,84
M35	Asn 220: HN-M35: O Asn 124: HN-M35: O Gln 123: HN-M35: N	Hydrogen bond Hydrogen bond Hydrogen bond	2.13 2.12 2.24	-9.46
M37	Gln 123: HN-M37: O Asn 220: HN-M37: O	Hydrogen bond Hydrogen bond	1.60 2.01	-7.85
MEROPENEM	Lys 211:HZ2-MEROPENEM: O Lys 211:HZ1-MEROPENEM: O Lys 211:HZ3-MEROPENEM: O Asn 220:HN-MEROPENEM: O Asn 220:HD22-MEROPENEM: O	Hydrogen bond Hydrogen bond Hydrogen bond Hydrogen bond Hydrogen bond	1.93 1.78 2.07 2.05 2.00	-9.19

Source: Self elaboration.

From the initial base of 22 compounds, M26 (-12.88 kcal/ mol with Autodock and -12.84 with Autodock$_{Zn}$) and M25 (-10.6 kcal/ mol with Autodock and -11.21 with Autodock$_{Zn}$) showed the lowest docking binding affinities to NDM-1 protein. Tables 1 and 2 show that the binding affinity values for the ligands M25, M35 and the reference antibiotic, Meropenem, improved against Autodock4, obtaining slightly lower results. These differences in binding values are due to the fact that Autodock$_{Zn}$ extends the AutoDock force field by including a specialized potential (potential that describes both the energetic and geometric components of the interaction), which includes the interactions of the coordination ligands with zinc, an aspect that may provide improvements compared to the AutoDock4 force fields, in parameters such as reproduction of the coordination geometry. These improvements brought by Autodock$_{Zn}$ are important in this work due to the fact that the nature of some ligands, in their activity against the receptor, are sought to increase interactions with zinc (Santos-Martins, D. et al., 2014).

3.2. ANALYSIS OF INTERMOLECULAR CONTACTS

As can be seen in Tables 1 and 2, as well as in Figure 3 (LigPlot diagrams), the NDM-1 residues involved in hydrogen bonds and hydrophobic interactions, with the molecules M26, M25, M37 and M35, as well as with the drug Meropenem, are shown. All the molecules with the best docking presented their docking in the active site reported for NDM-1, taking into account the reference amino acids coordinating with zinc atoms. Molecule M26, presents an approximate of 6 hydrogen bonds, highlighting those established with water molecule 303, which coordinates with zinc atoms, widely studied for being related to the hydrolysis mechanism of NDM, as well as with Zn 302. It also presents interactions with Glu 125, Asp 124, Asn 220 and Lys 211. It also presents important hydrophobic interactions with His 122, Gln 123, Trp93, Val 73, Gly 219, His 189 and Met 67 (Figure 3 A). On the other hand, molecule M25 presents two hydrogen bonds with the water molecule, as well as with Lys 211, and two hydrogen bonds with residue Asn 220. The hydrophobic interactions presented are Gly 219, Glu 152, Met 154, Gln 123, His 122, Met 67, Trp 93, Val 73, His 189 and Gly 219 (Figure 3 B). As for molecule M37, hydrogen bonds were present with residues Lys 211 and Asn 220 in addition to water molecule 303. Its hydrophobic order interactions were Val 73, Trp 93, Met 67, His 122, Gln 123, Asp 124, His 189, Leu 218, His 250 and Gly 219 (Figure 3 C). Finally, molecule M35 shows two hydrogen bonding interactions with residue Lys 211, one with Asn 220 and others with Met 67, Asp 124 and Gln 123. The hydrophobic interactions were Glu 152, Met 154, Leu 65, Val 73, Gly 219, Ser 217, Lys 211 His 250, Trp 93, His 122 and with water 303 (Figure 3 D).

A high number of hydrophobic interactions is highlighted in all structures of the 2D diagrams in Figure 3. Previous research has reported that hydrophobic interactions followed by hydrogen bonds are the interactions most closely linked to the stability of the protein-ligand complex structure (Kar, B. et al., 2023). It has also been proposed that increasing the number of hydrophobic interactions is favorable because the ligand structures are relatively smaller, so instead of satisfying geometrical constraints on electrostatic interactions, they benefit them (Kar, B. et al., 2023).

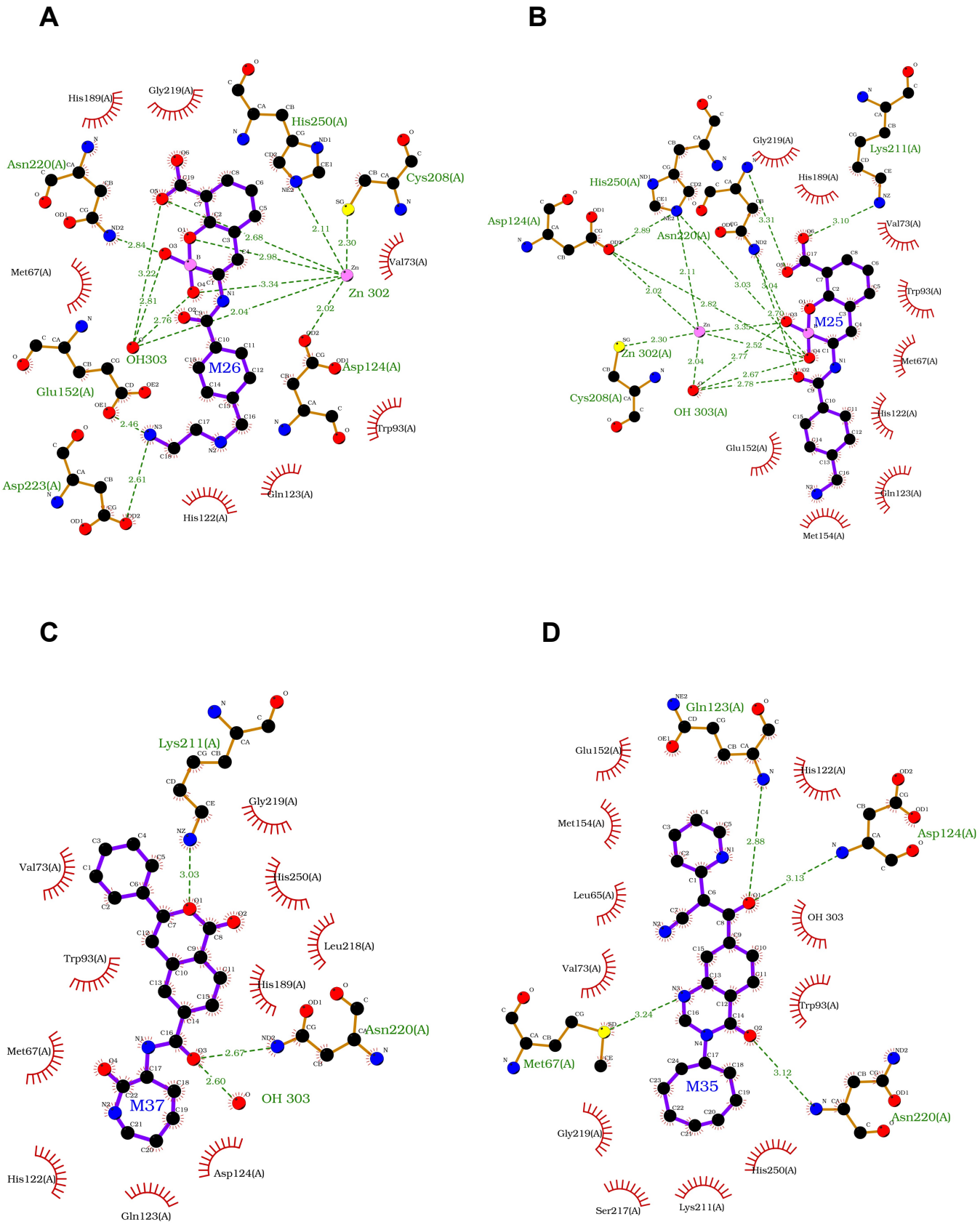

Figure 3. Ligplot diagrams showing interactions between NDM-1 residues and molecules A. M26, B. M25, C. M37 and D. M35 (Ball and stick model), residues in green are involved in hydrogen bonds and black in hydrophobic interactions.

3.3. ANALYSIS OF MOLECULAR DYNAMICS TRAJECTORIES

3.3.1. Analysis of the structural stability and compactness of the RMSD complex system.

Figure 4 shows that the protein backbone showed an initial deflection during the first 2 ns, which may be due to the stabilization of the initial protein structure. Subsequently, the system stabilized and showed a steady state dynamics trend specifically from 4ns onwards. The RMSD of the NDM-1 backbone fluctuated at values not exceeding 0.25nm , which, in fact, is within the recommended upper limit of 0.3nm. On the other hand, the RMSD of M26, which fitted into the backbone of NDM-1, fluctuates between 0.05nm and 0.275nm. The variation in the RMSD of compound M26 fitting into the backbone of NDM-1 could be due to the entry of ligand into the active site cavity of NDM- 1. Taken together, these results suggest the formation of a complex with relative stability, thus it could be thought that the ligand is stably bound to the binding site and does not diffuse out of the binding position.

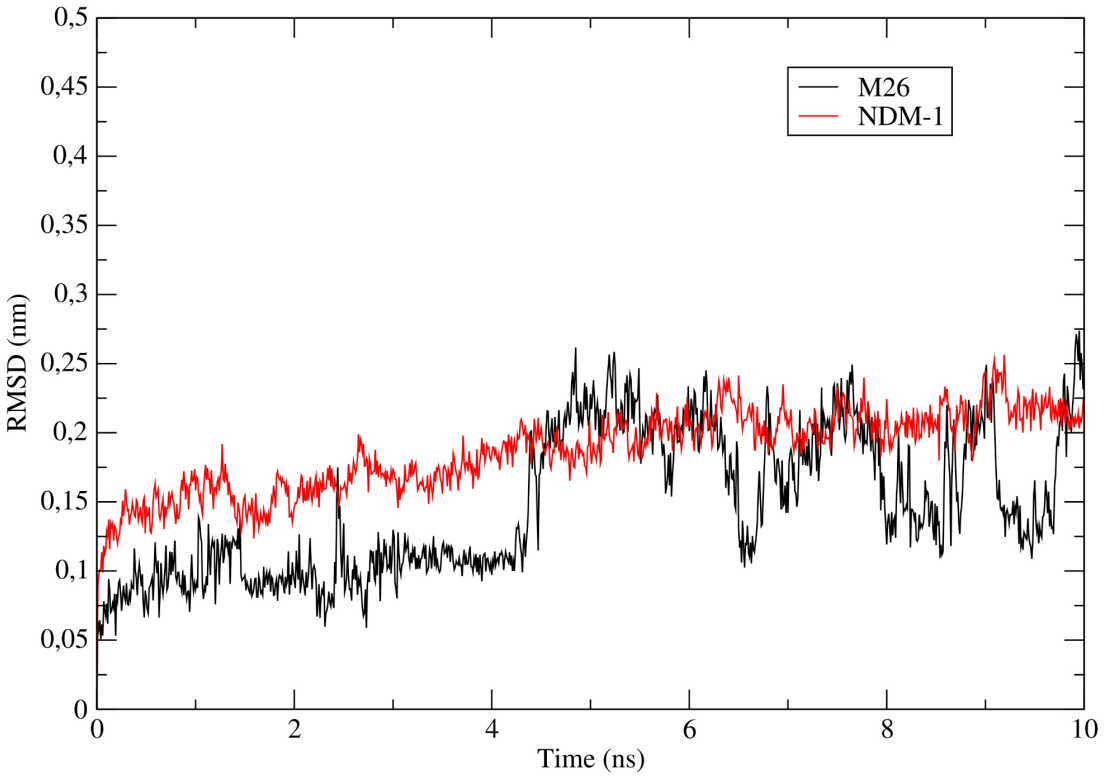

Figure 4 Molecular dynamics (MD) simulation of M26 with NDM-1 shows the root mean square deviations (RMSD) of NDM-1 alone and the NDM-1_M26 complex.

3.3.2. Structural flexibility analysis using RMSF data

In the RMSF calculation and diagram, the conformational flexibility of the NDM-1 protein was evaluated, where an approximate average variation during the trajectory from 0.02nm to 0.035nm is observed. In Figure 5, it is clearly evident that the fluctuations were minimal. No considerable peaks are observed in the area related to the active site (residues 120 to 250), this because the energy minimization process was efficient. This observation suggests that the protein was able to maintain its structural flexibility during the simulation.

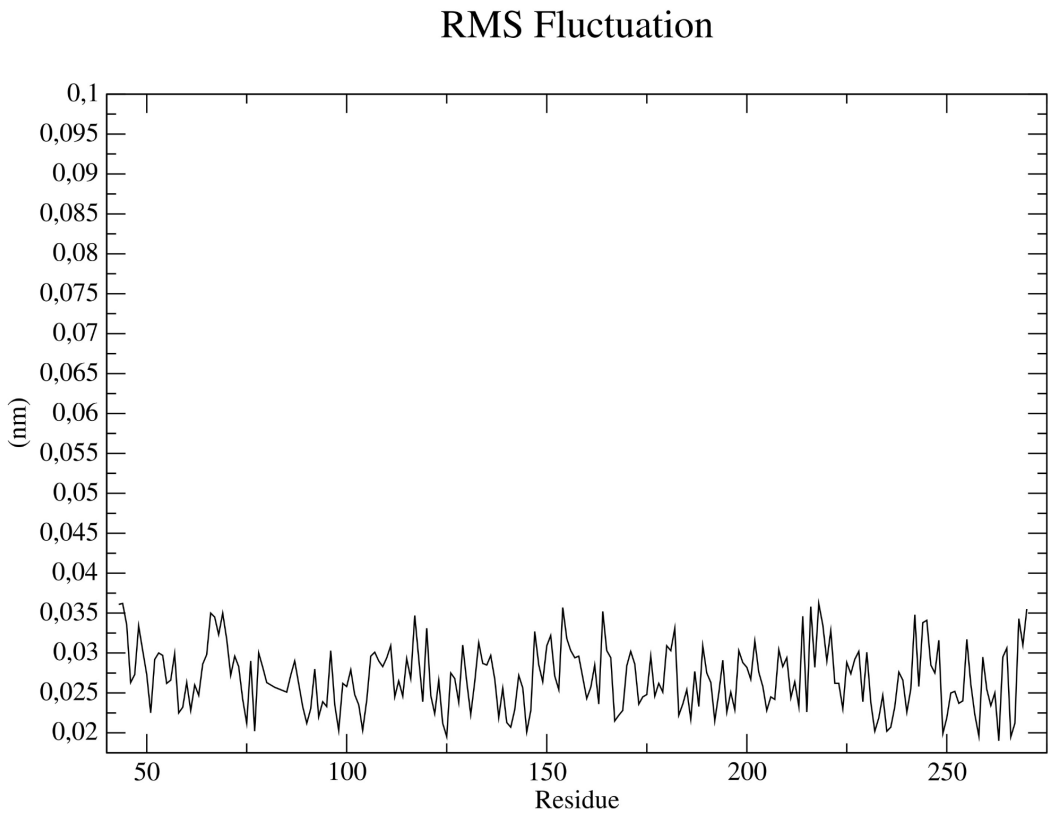

Figure 5. RMSF mean square fluctuation plot for a 10 ns period of MD simulations for NDM-1 protein residues.

4. FINAL CONSIDERATIONS

From a total of 22 initial compounds, the best molecular docking values were presented by molecules M26, M25, M27 and M35, respectively. It was possible to establish that the extended force field included in Autodock$_{Zn}$, produces some variations in the coupling values in comparison with Autodock4, in some cases, allowing to obtain even lower coupling results, i.e., it can improve the affinity values.

The analysis of the molecular contacts presented by the molecules M26 and M25 stand out due to their interaction with one of the two zinc atoms of NDM-1, crucial in

their catalytic activity, as well as with the water of the coordination site. Amino acids such as Lys 211, Gln 123, Trp 93, Val 73, Gly 219, and Met 67 were found to be relevant in stabilizing the ligand in the active site.

The RMSD trajectory analysis suggests the formation of a complex with relative stability. Similarly, RMSF analysis showed that the protein was able to maintain its structural flexibility during the simulation due to its few fluctuations, especially in the area related to the active site.

Author contributions

Eduvan Valencia and Wilson Olarte: Supervision and conceptualization. Eduvan Valencia, Wilson Olarte : revision and writing.

References

Alcaide, B., de Murga, R. M., Pardo, C., & Rodríguez-Ranera, C. (2004). Access to enantiopure polycyclic β-lactams by Diels–Alder reaction of novel inner-outer-ring 2-(silyloxy) dienes with a carbacepham skeleton. *Tetrahedron letters*, **45**, 7255-7259.

Ariza, B., & León, A. (2013). Carbapenemasa Nueva Delhi tipo 1 (NDM): Descripción fenotípica, epidemiológica y tratamiento. *Laboratorio Actual*, **44**.

Bebrone, C. (2007). Metallo-β-lactamases (classification, activity, genetic organization, structure, zinc coordination) and their superfamily. *Biochemical pharmacology*, *74*(12), 1686-1701.

Bernstein, F. C., Koetzle, T. F., Williams, G. J. B., Meyer, E. F., Brice, M. D., Rodgers, J. R., Kennard, O., Shimanouchi, T., & Tasumi, M. (1978). The protein data bank: A computer-based archival file for macromolecular structures. Archives of Biochemistry and Biophysics, 185(2), 584–591.

Cruz, E., & Ramón, G. (2010). Modelación molecular de antibióticos betalactámicos. *Medisur*, **8**, 13-19.

Deshpande, P., Rodrigues, C., Shetty, A., Kapadia, F., Hedge, A., & Soman, R. (2010). New Delhi Metallo-beta lactamase (NDM-1) in Enterobacteriaceae: treatment options with carbapenems compromised. *The Journal of the Association of Physicians of India*, **58**, 147-149.

Etruri, B., Jardini, A., & Maciel R., (2021) In silico evaluation of most used drugs on the treatment of slight and mild covid-19 cases in Brazil, International Journal of Development Research, 11, (06), 48146-48150.

Gonzalez *et al*., (2015), Caracterización fenotípica y genotípica de perfiles de resistencia antimicrobiana de aislamientos bacterianos recuperados en Infecciones Asociadas a la Atención en Salud (IAAS) septiembre 2012 - diciembre 2014. [En

línea]. Instituto nacional de salud, Bogotá, Colombia. [Consultado en agosto de 2022]. Disponible en: https://www.ins.gov.co/buscador/Informacin%20de%20laboratorio/Informe%20Vigilancia%20por%20Laboratorio%20Resistencia%20Antimicrobiana%20IAAS%202012-2014.pdf

Goodsell, D. S., Morris, G. M., & Olson, A. J. (1996). Automated docking of flexible ligands: applications of AutoDock. *Journal of molecular recognition*, *9*(1), 1-5.

Guo, Y., Wang, J., Niu, G., Shui, W., Sun, Y., Zhou, H., ... & Rao, Z. (2011). A structural view of the antibiotic degradation enzyme NDM-1 from a superbug. *Protein & cell*, **2**, 384-394.

Haque, M. A., Marathakam, A., Rana, R., Almehmadi, S. J., Tambe, V. B., Charde, M. S., ... & Khan, S. L. (2023). Fighting Antibiotic Resistance: New Pyrimidine-Clubbed Benzimidazole Derivatives as Potential DHFR Inhibitors. *Molecules*, *28*(2), 501.

Kar, B., Kundu, C. N., Pati, S., & Bhattacharya, D. (2023). Discovery of phyto-compounds as novel inhibitors against NDM-1 and VIM-1 protein through virtual screening and molecular modelling. *Journal of Biomolecular Structure and Dynamics*, *41*(4), 1267-1280.

Liu, X. L., Shi, Y., Kang, J. S., Oelschlaeger, P., & Yang, K. W. (2015). Amino acid thioester derivatives: a highly promising scaffold for the development of metallo-β-lactamase L1 inhibitors. *ACS medicinal chemistry letters*, **6**, 660-664.

Morales-Moreno, Y., Medina-Marrero, R., Garcia-Bernal, M., Casanova-González, M., Rodríguez-Pérez, R., Fernández-López, N., ... & Rojas-Hernández, N. (2014). Actividad in vitro de furvina frente a bacterias Gram negativas multirresistentes. *Revista CENIC. Ciencias Biológicas*, **45**, 052-057.

Murray, C. J., Ikuta, K. S., Sharara, F., Swetschinski, L., Aguilar, G. R., Gray, A., ... & Naghavi, M. (2022). Global burden of bacterial antimicrobial resistance in 2019: a systematic analysis. *The Lancet*, **399**, 629-655.

Papp-Wallace, K. M., Endimiani, A., Taracila, M. A., & Bonomo, R. A. (2011). Carbapenems: past, present, and future. *Antimicrobial agents and chemotherapy*, **55**, 4943-4960.

Queenan, A., & Bush, K. (2007). Carbapenemases: the versatile β-lactamases. *Clinical microbiology reviews*, **20**, 440-458.

Rehman, M. T., AlAjmi, M. F., Hussain, A., Rather, G. M., & Khan, M. A. (2019). High-throughput virtual screening, molecular dynamics simulation, and enzyme kinetics identified ZINC84525623 as a potential inhibitor of NDM-1. *International journal of molecular sciences*, *20*(4), 819.

Salih, T., & Ali, P. G. (2023). Rational design of novel compounds to serve as potential NDM-1 inhibitors using molecular docking, molecular dynamics simulation, and physicochemical studies.

Santos-Martins, D., Forli, S., Ramos, M. J., & Olson, A. J. (2014). AutoDock4Zn: an improved AutoDock force field for small-molecule docking to zinc metalloproteins. *Journal of chemical information and modeling*, *54*(8), 2371-2379.

Suárez, C., & Gudiol, F. (2009). Antibióticos betalactámicos. *Enfermedades infecciosas y microbiología clínica*, **27**, 116-129.

Van Der Spoel, D., Lindahl, E., Hess, B., Groenhof, G., Mark, A. E., & Berendsen, H. J. (2005). GROMACS: fast, flexible, and free. *Journal of computational chemistry*, *26*(16), 1701-1718.

Xiong, G., Wu, Z., Yi, J., Fu, L., Yang, Z., Hsieh, C., ... & Cao, D. (2021). ADMETlab 2.0: an integrated online platform for accurate and comprehensive predictions of ADMET properties. *Nucleic Acids Research*, *49*(W1), W5-W14.

Yacoby, I., & Benhar, I. (2007). Targeted anti bacterial therapy. *Infectious Disorders-Drug Targets (Formerly Current Drug Targets-Infectious Disorders)*, **7**, 221-229.

Yang, S. K., Kang, J. S., Oelschlaeger, P., & Yang, K. W. (2015). Azolylthioacetamide: a highly promising scaffold for the development of metallo-β-lactamase inhibitors. *ACS medicinal chemistry letters*, **6**, 455-460.